Analytical Modeling of Electromagnetic Noise in Spoke-Type Permanent-Magnet Machines

Lazhar ROUBACHE
Laboratoire de Recherche en Electrotechnique (LRE)
Ecole Nationale Polytechique (ENP)
El-Harrach, Algérie
lazhar.roubache@g.enp.edu.dz

Mohammed BEN YAHIA
Laboratoire de Recherche en Electrotechnique (LRE)
Ecole Nationale Polytechique (ENP)
El-Harrach, Algérie
mohammed.ben_yahia @g.enp.edu.dz

Kamel BOUGHRARA
Laboratoire de Recherche en Electrotechnique (LRE)
Ecole Nationale Polytechique (ENP)
El-Harrach, Algérie
kamel.boughrara@g.enp.edu.dz

Frédéric DUBAS
Département ÉNERGIE, FEMTO-ST, CNRS
Univ. Bourgogne Franche-Comté
F90000 Belfort, France
FDubas@gmail.com

Rachid IBTIOUEN
Laboratoire de Recherche en Electrotechnique (LRE)
Ecole Nationale Polytechique (ENP)
El-Harrach, Algérie
rachid.ibtiouen@gmail.com

***Abstract*—This paper presents an analytical modeling of electromagnetic noise in spoke-type permanent-magnet (PM) machines (STPMMs). The two-dimensional (2-D) elementary subdomain (E-SD) technique in polar coordinates is used to predict the magnetic pressure, which is transferred to frequency domain and used in harmonic response mechanical analysis to predict generated electromagnetic noise. An electro-vibro-acoustic coupling based on a 2-D finite-element method (FEM) has been realized in order to validate the obtained results by the analytical modeling.**

Keywords—Analytical; electrical machines; noise; elementary subdomain technique; pressure; numerical.

I. Introduction

The magnetic field in the air-gap between the stator and rotor in electrical machines generates tangential forces required for producing the rotating torque. In addition, this magnetic field also produces radial forces that interact with the machine structure and create the vibration and/or noise (i.e., electromagnetic noise). In high-speed electrical machines, the frequencies of these forces become near to natural frequencies of the machine structure, and thus the produced noise become more important. In the last decade, several works have treated this type of noise for different types of electrical machines **[1]-[3]**.

The first step in electromagnetic noise prediction is the determination of magnetic field inside the machine. This can be done by using numerical methods (e.g., FEM) **[4]-[5]** or semi-analytical method (e.g., SD technique or magnetic equivalent circuit) **[1]-[2]** and **[6]**. Using Maxwell stress tensor, the radial pressure can be defined from the magnetic field in the air-gap. Then, these temporal results should be transformed into frequency domain using 2-D Fast Fourier Transformation (FFT). This transition makes the radial forces as waves have specified temporal frequency and spatial order. Then, the superposition study is done to determine the produced deformation for each wave. This harmonic response analysis need the naturel frequencies determination of machine structure that can be determined by using FEM or analytic approaches **[7]**.

This paper presents a description of coupled electro-vibro-acoustic model for STPMMs. The electromagnetic analysis is performed by using the 2-D E-SD technique in polar coordinates where the local saturation effect is taken into account with the *B(H)* curve **[8]**. Then, the produced electromagnetic noise is predicted by using analytical vibro-acoustic approach **[1]**. The obtained results are validated by 2-D electro-vibro-acoustic FEM.

II. Electromagnetic Model

A. 2-D E-SD Technique

The SD technique is one of the most resent semi-analytical methods for magnetic field prediction in electrical machines. Some comprehensive reviews for this method can be found in **[9]-[12]**. Recently, an improvement of this technique by focusing on the consideration of local saturation effect with the *B(H)* curve is done in **[8]**. In this model, the rotor and the stator are divided into E-SD characterized by general solution to first harmonic of magnetostatic Maxwell's equation. Then, as **[12]**, the connection is performed in both directions (i.e., *r*- and θ- edges). The simulation is done for successive moment where the rotor position and stator currents (i.e., sinusoidal supply) are updated for each time. The obtained results are validated by 2-D transient FEM. The simulation machine and its parameters are shown in **Fig. 1** and **Table. I**.

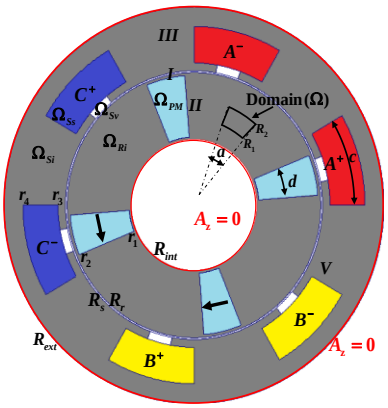

Fig. 1. Examples of STPMM **[8]**.

TABLE I. PARAMETERS OF STUDIED MACHINE.

Symbol	Parameters	Value and Units
B_{rm}	Remanent flux density of PMs	1.2 *T*
μ_{rm}	Relative permeability of PMs	1
N_c	Number of conductors per stator slot	200
I_m	Peak phase current	10 *A*
Q_s	Number of stator slots	6
c	Stator slot-opening	30 *deg.*
c_r	Stator isthmus-opening	10 *deg*
d	PM-opening	18 *deg.*
p	Number of pole pairs	2
R_{ext}	Radius of the external stator surface	67 *mm*
r_4	External radius of stator slot	60.3 *mm*
r_3	Internal radius of stator slot	48 *mm*
R_s	Radius of the internal stator surface	45.3 *mm*
R_r	Radius of the external rotor surface	44.8 *mm*
r_2	External radius of the PMs	43.8 *mm*
r_1	Internal radius of the PMs	23 *mm*
R_{int}	Radius of the rotor inner surface	22 *mm*
L_u	Axial length of machine	63 *mm*
Ω	Mechanical pulse of synchronism	3,750 *rpm*

In **Fig. 2**, a comparison between the numerical results and semi-analytical predictions are shown in term of $\boldsymbol{B}$ in the middle of the air-gap (i.e., $r = R_e$) versus angular position. The r- and θ-component of $\boldsymbol{B}$ for the position $(R_e, 0)$ versus time is presented in **Fig. 3**.

B. Magnetic Pressure and Harmonic Formulation

Using Maxwell stress tensor, the space and time distribution of radial magnetic pressure can be computed by **[6]**

$$P_{rad}(t,\theta) = \frac{B_r^2(t,\theta) - B_\theta^2(t,\theta)}{2\mu_0} \quad (1)$$

where B_r and B_θ are the r- and θ-component of $\boldsymbol{B}$ in the middle of the air-gap. The obtained analytical results are shown in **Fig. 4**. It should be noted that the radial magnetic pressure prediction can be calculated with others analytical methods such as magnetomotive force method.

The harmonics of pressure are obtained by performing a 2-D FFT of the space and time pressure distribution, viz.,

$$P_{rad}(t,\theta) = \sum P_{rf} e^{j(2\pi ft - r\theta + \varphi_{fr})} \quad (2)$$

where f, r, P_{rf}, φ_{fr} are respectively the frequency, the order, the magnitude and the phase for each pressure harmonic. **Fig. 5** presents the magnitude of each harmonic and mode (f, r).

III. VIBRO-ACOUSTIC SYNTHESIS

The mechanical model assumes that the stator is a 2-D ring with free-free boundary conditions. Therefore, only in-plane circumferential spatial modes r are considered.

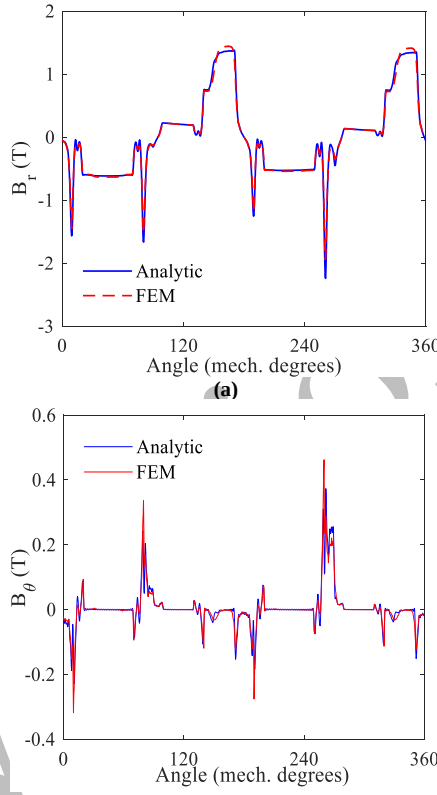

Fig. 2. Waveform of $\boldsymbol{B}$ in the middle of the air-gap for on load condition with I_m = 10 *A*: **(a)** r- and **(b)** θ-component.

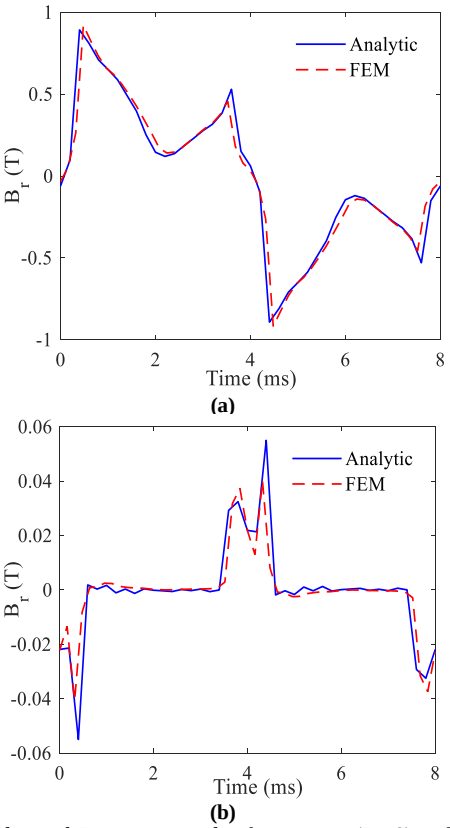

Fig. 3. Waveform of $\boldsymbol{B}$ versus time for the position (R_e, 0) and for on load condition I_m = 10 *A*: **(a)** r- and **(b)** θ-component.

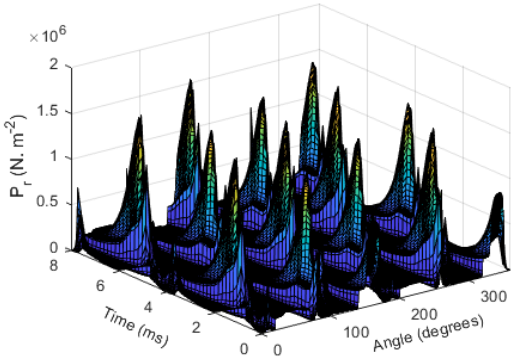

Fig. 4. Analytical radial magnetic pressure on load condition.

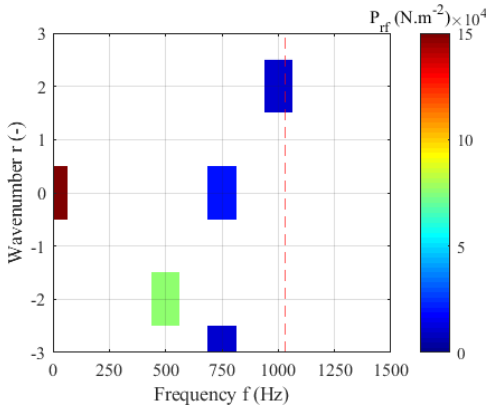

Fig. 5. 2-D FFT of radial magnetic pressure at on-load condition.

A. *Mode Shape and Natural Frequency*

For predicting the vibrations originating from the stator, it is necessary to calculate the natural frequency of each vibration mode shape. Here, the mechanical system of the stator was considered as a cylinder for calculating the natural frequency. At this time, the mode shape of the mechanical vibration occurs only in the circumferential direction. The natural frequency f_r of the r^{th} mode shape is expressed as follows **[7]**:

- for the fundamental mode (i.e., $r = 0$):

$$f_0 = \frac{1}{2\pi R_c}\sqrt{\frac{E_c}{\rho_c k_{md}}} \quad \text{with } k_{md} = \frac{M_c + M_t}{M_c} \tag{3}$$

- for the harmonic modes (i.e., $r > 1$):

$$f_r = f_0 \Gamma \frac{r(r^2-1)}{\sqrt{r^2+1}} \quad \text{with } \Gamma^2 = \frac{h_t^2}{12R_c^2} \tag{4}$$

where R_c is the stator mean radius, h_t the yoke depth, L_u the axial length of machine, k_{md} the mass increase factor due to teeth, M_t is the teeth mass, M_c is the stator yoke mass, E_c the Young's module (i.e., $E_c = 200\ MPa$), and ρ_c the stator stack mass density (i.e., $\rho_c = 7{,}850\ kg/m^3$). It should be noted that the first mode is not considered in stator structure deformation. In fact, this mode is approximated as treating the rotor structure **[2]**.

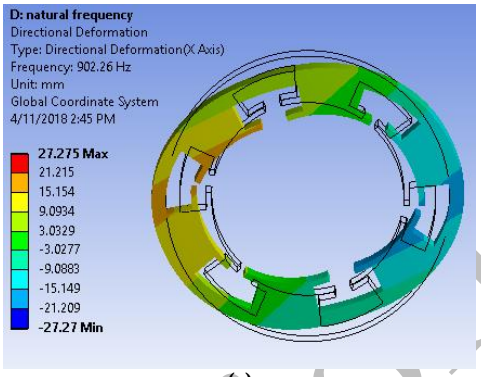

(a)

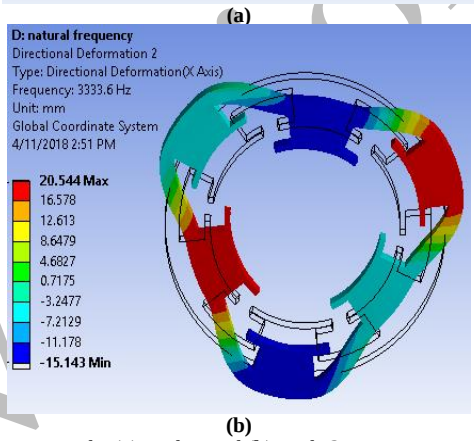

(b)

Fig. 6. Harmonic mode: **(a)** mode 2 and **(b)** mode 3.

TABLE II. NATURAL FREQUENCY.

Mode r	Analytic [Hz]	FEM [Hz]
0	9,819.2	-
2	1,082.4	902.2
3	3,203.1	3,333.6

The modes 2 and 3 are shown in **Fig. 6**. The natural frequencies obtained analytically and by FEM are shown in **Table. II**.

B. *Stator Radial Deformation*

The amplitude of vibration displacement of mode r can be calculated as **[2]**

$$A_r = \frac{12R_a R_c^3}{E_c h_t^3 \left(r^2-1\right)^2} P_{rf} h_r \tag{5}$$

$$h_r = \frac{1}{\sqrt{\left(1-\frac{f}{f_r}\right)^2 + \left(2\zeta_r \frac{f}{f_r}\right)^2}} \tag{6}$$

$$\zeta_r = \frac{1}{2\pi}\left(2.76\times10^{-5} f_r + 0.062\right) \tag{7}$$

where R_a is the stator bore radius.

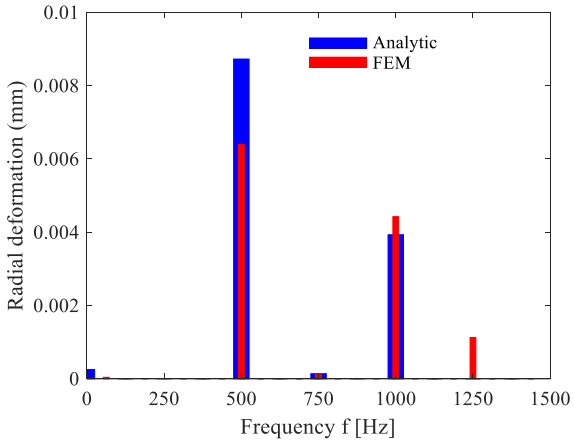

Fig. 7. Radial deformation at the external stator surface.

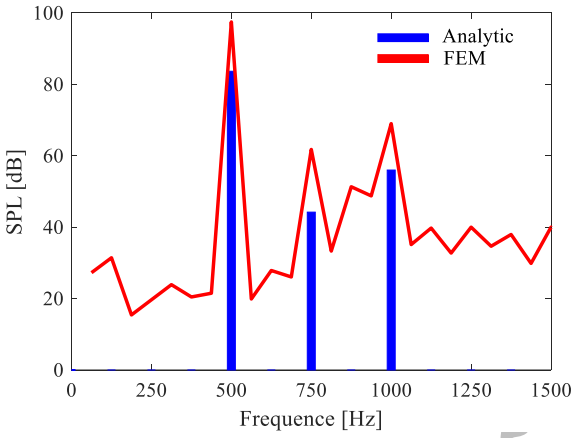

Fig. 8. Sound power level at the external stator surface.

The vibration velocity for the mode *r* is:

$$V_r = 2\pi f A_r \tag{8}$$

Fig. 7 shows the maximum radial deformation at the external stator surface. It can be seen that the deformation at the frequency $f = 1,000\ Hz$ is important despite the low value of the corresponding harmonic pressure as this frequency is near to the natural frequency of the second mode [see **Fig. 5**].

C. Acoustic Model

The radiated sound power from the stator outer surface for mode m can calculated as [2]

$$W_r(f) = \rho_0 c_0 S_c \sigma_r \left(\frac{V_r}{\sqrt{2}}\right)^2 \tag{9}$$

where $S_c = \pi R_{ext} L_u$ is the stator outer surface with R_{ext} the radius of the external stator surface and L_u the axial length of machine, $\rho_0 = 1.188\ \text{kg/m}^3$ the air density, $c_0 = 344\ \text{m/s}$ the sound speed in the air-gap, and σ_r the modal radiation efficiency.

The sound power level (SPL) at frequency *f* is

$$L_r(f) = 10\log_{10}\left(\sum_r \frac{W_r}{W_0}\right) \tag{10}$$

with $W_0 = 10^{-12} W$ the reference sound power.

Fig. 8 shows the SPL radiation. On can see the tow pick at 500 *Hz* and 1,000 *Hz*, which are corresponding to the second mode. The pick at 750 *Hz* has less magnitude as the natural frequency at this mode is greater (i.e., $f_r = 3,333.6\ Hz$).

IV. Conclusion

An analytical model has been developed to determine radial deformation and electromagnetic noise in STPMMs. The magnetic pressure has been calculated by using the 2D E-SD technique in polar coordinates. Then, the harmonics of magnetic pressure are used to estimate the generated displacement and noise. The obtained results are validated by FEM.

The coincide of the harmonic pressure frequency with the natural frequency of the corresponding mode can generate important deformation indeed important SPL. Furthermore, the electromagnetic noise is important in high-speed machines.

References

[1] J.F. Gieras, J.C. Lai, and C. Wang, *Noise of Polyphase Electric Motors*. Boca Raton, FL: CRC/Taylor & Francis, 2006.

[2] J. Le Besnerais, V. Lanfranchi, M. Hecquet, P. Brochet, and G. Friedrich, "Acoustic noise of electromagnetic origin in a fractional-slot induction machine," *COMPEL - The international journal for computation and mathematics in electrical and electronic engineering*, vol. 27, no. 5, pp. 1033-1052, Dec. 2008.

[3] R. Islam, and I. Husain, "Analytical model for predicting noise and vibration in permanent magnet synchronous motors," in *Proc. ECCE*, San Jose, CA, USA, Sep. 20-24, 2009.

[4] I-S. Jang, S-H. Ham, W-H. Kim, C-S. Jin, S-Y. Cho, K-D. Lee, J-J. Lee, D. Kang, and J. Lee, "Method for analyzing vibrations due to electromagnetic force in electric motors," *IEEE Trans. Magn.*, vol. 50, no. 2, Feb. 2014, Art. ID: 7007204.

[5] A. Saito, H. Suzuki, M. Kuroishi, and H. Nakai, "Efficient forced vibration reanalysis method for rotating electric machines," *Journal of Sound and Vibration*, vol. 334, pp. 388-403, Jan. 2015.

[6] E. Devillers, M. Hecquet, J.L. Besnerais, and M. Regniez, "Tangential effects on magnetic vibrations and acoustic noise of induction machines using subdomain method and electromagnetic vibration synthesis," in *Proc. IEMDC*, Miami, FL, USA, May 21-24, 2017

[7] J-P. Lecointe, R. Romary, J-F. Brudny, and T. Czapla, "Five methods of stator natural frequency determination: case of induction and switched reluctance machines," *Mechanical Systems and Signal Processing*, vol. 18, no. 5, pp. 1133-1159, Sep. 2004.

[8] L. Roubache, K. Boughrara, F. Dubas, and R. Ibtiouen, "Elementary subdomain technique for magnetic field calculation in rotating electrical machines with local saturation effect," *COMPEL - The international journal for computation and mathematics in electrical and electronic engineering*, **To be published**, 2018.

[9] F. Dubas, and C. Espanet, "Analytical solution of the magnetic field in permanent-magnet motors taking into account slotting effect: No-load vector potential and flux density calculation," *IEEE Trans. Magn.*, vol. 45, no. 5, pp. 2097-2109, May 2009.

[10] Z.Q. Zhu, L.J. Wu, and Z.P. Xia, "An accurate subdomain model for magnetic field computation in slotted surface-mounted permanent-

magnet machines," *IEEE Trans. Magn.*, vol. 46, no. 4, pp. 1100-1115, Apr. 2010.

[11] E. Devillers, J. Le Besnerais, T. Lubin, M. Hecquet, and J.P. Lecointe, "A review of subdomain modeling techniques in electrical machines: Performances and applications," in *Proc. ICEM*, Lausanne, Switzerland, Sep. 04-07, 2016.

[12] F. Dubas, and K. Boughrara, "New scientific contribution on the 2-D subdomain technique in Cartesian coordinates: Taking into account of iron parts," *Math. Comput. Appl.*, vol. 22, no. 1, p. 17, Feb. 2017, DOI: 10.3390/mca22010017.